Association of a Triblock Ethylene Oxide (E) and Butylene Oxide (B) Copolymer ($B_{12}E_{260}B_{12}$) in Aqueous Solution

Zukang Zhou,[†] Yung-Wei Yang,[‡] Colin Booth,[‡] and Benjamin Chu*[,†]

Department of Chemistry, State University of New York at Stony Brook, Stony Brook, New York 11794−3400, and Manchester Polymer Center, Department of Chemistry, University of Manchester, Manchester M13 9PL, UK

Received May 21, 1996; Revised Manuscript Received September 20, 1996[⊗]

ABSTRACT: The association behavior of a triblock ethylene oxide (E) and butylene oxide (B) copolymer with a very long middle E block ($B_{12}E_{260}B_{12}$) in aqueous solution has been investigated by means of laser light scattering. The flower-like closed association behavior of BEB−type triblock copolymers in aqueous solution can be altered to form open, branched, associated structures because of the very long E blocks. The $B_{12}E_{260}B_{12}$ triblock forms flower-like micelles in a closed association process with a critical micelle concentration of 0.056, 0.040, and 0.033 mg/mL even at fairly low temperatures of 10.0, 20.0, and 25.0 °C, respectively. At room temperature, $B_{12}E_{260}B_{12}$ can form large secondary associated structures which coexist with the flower-like micelles at concentrations of only 1−2% (w/v). The secondary associates increase in both amount and size with increasing concentration and increasing temperature, producing a highly viscous fluid even for a 4% aqueous solution of $B_{12}E_{260}B_{12}$.

Introduction

Studies of the micellization of water-soluble triblock copolymers have been carried out extensively[1−6] using $E_mP_nE_m$, where E and P represent, respectively, oxyethylene and oxypropylene units. An in-depth review of the physical chemistry of polyoxyalkylene block copolymers in aqueous solution has recently appeared.[7] $E_mP_nE_n$ triblocks form essentially core−shell micelles in aqueous media and obey a closed association process. A limited range of triblock $P_nE_mP_n$ copolymers are available commercially. $P_nE_mP_n$ triblocks tend to form flower-like micelles in aqueous media.[8] A profound effect on the critical micelle concentration (cmc) has been detected by changing the molecular architecture from $E_mP_nE_m$ to $P_nE_mP_n$ with comparable chain length and composition. For example, the cmc of $E_{13}P_{30}E_{13}$ is 0.9 mg/mL, while that of $P_{14}E_{24}P_{14}$ is 91 mg/mL at 40 °C.[8] Furthermore, extended structures due to the self-assembly of $P_nE_mP_n$ triblocks are possible, as the micellar association may not necessarily involve copolymer chains with both end blocks in the *same* core (forming loops for the middle blocks and resulting in flower-like micelles) but also with one end block in the core and the other in the dangling fringe. The open structure formed by the fringes could link up with other micelles via copolymer chains or via end block fringes by means of intermicellar association. Such open structures for triblocks have been predicted[9,10] and observed experimentally in organic[11] and aqueous[12] solvents. For example, $P_{15}E_{156}P_{15}$ with a lengthy E block was shown to form network structures linked by micellar associates.

Replacement of propylene oxide (P) by 1,2-butylene oxide (B) provides more hydrophobicity, which enhances association in dilute solution even with very short end blocks,[13] e.g., from B_4 to B_8. In aqueous solution at 40 °C, cmc = 0.3 and 30 mg/mL for $E_{41}B_8$ and $B_4E_{40}B_4$ copolymers, respectively, showing again the significant effect of the block sequence on the micellization ability. A few $E_mB_nE_m$ copolymers are available from the Dow Chemical Co.[14] However, $B_nE_mB_n$ triblocks are not yet readily available. The association behavior of $B_4E_{40}B_4$, $B_5E_{39}B_5$, and $B_7E_{40}B_7$ in aqueous solution has been investigated by laser light scattering.[15] In the above series, the overall chain length and the composition remain essentially the same while the hydrophobicity of the end blocks changes from B_4 to B_7. Experimental results suggested the existence of small molecular associates, micelles, and bridged-micelle clusters. A related study[16] of the micellar association of triblock copolymer $B_{12}E_{76}B_{12}$ mixed with diblock copolymer $E_{41}B_8$ provided a means of control over the micelle/bridged-micelle equilibrium. In the present work, we increase the length of the middle E block with $m = 260$ and $n = 12$ for the $B_nE_mB_n$ triblock copolymer. The specific purpose is to examine whether flower-like closed association behavior occurs and can undergo a transition to an open, branched association mechanism when the middle E chain is so long.

Experimental Section

Preparation and Characterization of Copolymer. The copolymer ($B_{12}E_{260}B_{12}$) was prepared by sequential anionic polymerization of ethylene oxide and 1,2−butylene oxide. All reagents were distilled and dried before use. Polymerization was carried out using vacuum line and ampule techniques in order to minimize initiation by moisture. The initiator solution was prepared by reacting freshly cut potassium with diethylene glycol at a ratio [OH]/[OK] ≈ 9. The details have been described elsewhere.[13]

The sample was characterized by gel permeation chromatography, consisting of four μ−Styragel columns, and nuclear magnetic resonance spectroscopy using a Varian Unity 500 spectrometer operated at 125.5 MHz. The procedure has been described elsewhere.[15] It is noted that the copolymer was further purified by extraction with warm hexane in order to remove small quantities of homopoly(oxybutylene) which had been initiated by introduction of small amounts of moisture with the second monomer.

Cloud-Point Determination. The cloud point was determined by monitoring the transmitted intensity from a low-powered He−Ne laser beam. The cloud point was determined as the midpoint of an abrupt decrease in the transmitted light intensity from a plot of transmitted intensity versus temperature. When coming nearer to the clouding temperature, the temperature of the copolymer solution was raised slowly at about 0.1 °C/min.

[†] State University of New York at Stony Brook.
[‡] University of Manchester.
[⊗] Abstract published in *Advance ACS Abstracts,* November 1, 1996.

S0024-9297(96)00747-4 CCC: $12.00

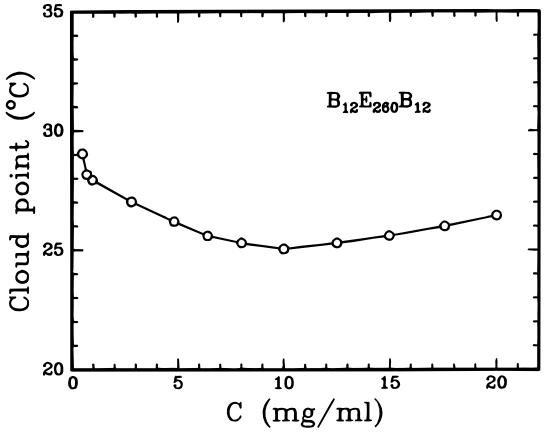

Figure 1. Plot of cloud-point temperature versus concentration for $B_{12}E_{260}B_{12}$. A shallow minimum at ~25 °C and 10 mg/mL is observed.

Static and Dynamic Light Scattering. A standard, laboratory-built light-scattering spectrometer,[17] functioning as photon-counting equipment, with a Spectra Physics Model 165 argon ion laser operating at 488 nm and a Brookhaven Instruments (BI 2030AT or BI9000) correlator were used to measure static and dynamic light scattering. The sample chamber was thermostated and could be controlled to within ±0.02 °C. Benzene was used as a reference standard. The intensity−intensity time correlation functions were analyzed by means of CONTIN method.[18]

Results and Discussions

The self-assembly process for block copolymers in selective solvents can be initiated either by an increase in concentration via the cmc or by changing the temperature via the critical micelle temperature (cmt). After micelle formation, at elevated temperatures the polymer solution can undergo another phase transition, such as liquid−liquid phase separation of the binary fluid mixture. The self-assembly behavior can be described as follows.

1. Cloud-Point Curve. Figure 1 shows a plot of cloud-point temperature as a function of concentration for $B_{12}E_{260}B_{12}$. The cloud-point curve exhibited a shallow minimum at ~25 °C and 10 mg/mL. In the one-phase region, the cmcs at temperatures of 10, 20, and 25 °C were found to be less than 0.1 mg/mL. Thus, the cloud-point behavior represented the phase transition of a solution of copolymer micelles. Reference 16 gives the following clouding temperature data (1% solution): $B_4E_{40}B_4$ at 61 °C, $B_5E_{39}B_5$ at 43 °C, $B_7E_{40}B_7$ at 26 °C, and $B_{12}E_{76}B_{12}$ at 12 °C. Reference 19 gives $B_{12}E_{114}B_{12}$ at 17 °C. A 1% $B_{12}E_{260}B_{12}$ shows a cloud point of 25 °C. Thus, the B-block length has much greater influence on the clouding temperature than the E-block length.

2. Dilute Solution Region (C < 1 mg/mL). In the dilute solution region, the micellization behavior, including the hydrodynamic radius (R_h), the weight-average aggregation number (n_w), and the second virial coefficients (A_2 and k_D) can be determined by means of static light scattering (SLS, with A_2 being the second virial coefficient) and dynamic light scattering (DLS, with k_D being the diffusion second virial coefficient).

Static Light Scattering. Figure 2 shows a plot of $I/I_{bz,25}$ versus concentration (C) at 10.0, 20.0, and 25.0 °C. The excess scattered intensity (I) is essentially independent of scattering angle because of the small unimer and micellar sizes. $I_{bz,25}$ is the reference standard (benzene) measured at 25.0 °C. SLS experiments were performed at concentrations of less than 1 mg/mL. The sharp increase in the scattered intensity could be

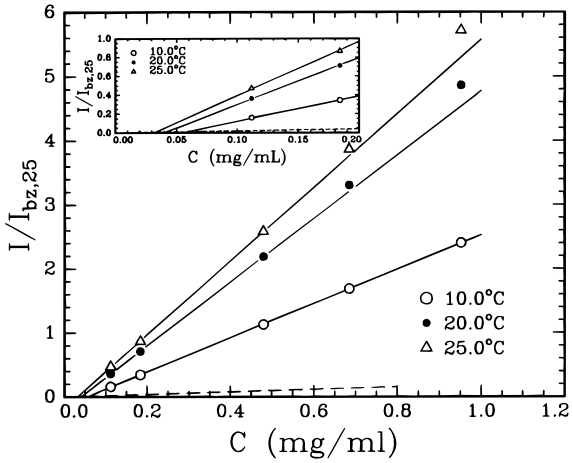

Figure 2. Plot of $I/I_{bz,25}$ versus concentration for $B_{12}E_{260}B_{12}$ at 10.0, 20.0, and 25.0 °C. $I/I_{bz,25}$ denotes the normalized excess scattered intensity with $I_{bz,25}$ being the scattered intensity of the reference standard (benzene) at 25 °C. The inset represents the same plot with emphasis in the very dilute region in order to determine the cmc at 10.0, 20.0, and 25.0 °C.

extrapolated back to $I/I_{bz,25} \approx 0$, where the contribution of $I/I_{bz,25}$ by the unimers at initial concentrations of less than ~0.06 mg/mL is essentially negligible. The dashed line in Figure 2 represents the $I/I_{bz,25}$ values of triblock unimers in ideal solutions, where the second virial coefficient $A_2 = 0$. The intersections are the cmcs. The inset in Figure 2 shows that the cmc values obtained from SLS are 0.056, 0.040, and 0.033 mg/mL at 10.0, 20.0, and 25.0 °C, respectively. The uncertainties in the cmc values obtained were estimated to be ±4.0%, ±4.5%, and ±9.5%, respectively. Note that the cmc values for $B_5E_{91}B_5$ are much larger, i.e., 12.4, 4.4, and 1.6 mg/mL at 25.0, 35.0, and 45.0 °C, respectively, as reported elsewhere.[20] Figure 3a shows a plot of the reciprocal of the relative reduced scattered intensity $C/(I/I_b)$ versus concentration as a function of copolymer concentration at 10.0, 20.0, and 25.0 °C. The upturn at low concentrations, which becomes weaker with increasing temperature, reflects the extent of micellar dissociation. Figure 3b shows the corresponding reduced scattered intensity (KC_{mic}/R_{mic} in mol/g) as a function of micellar concentration (C_{mic}). The micellar concentration was very close to the initial concentration because of the low cmc values. The weight average molar mass (M_w) of the micelle and the second virial coefficient (A_2) were obtained by the relation

$$\frac{KC_{mic}}{R_{mic,90}} = \frac{1}{M_w} + 2A_2C_{mic} \qquad (1)$$

where K ($=4\pi n_o^2(dn/dC)^2/(N_A\lambda_o^4)$) is an optical constant with N_A, n_o, and λ_o being Avogadro's number, the solvent refractive index, and the wavelength of light in vacuo, respectively. $R_{mic,90}$ is the excess Rayleigh ratio by micelles at a scattering angle 90° with vertically polarized incident and scattered light beams. The dn/dC value (=0.133 cm^3 g^{-1} at 30 °C) and its temperature coefficient (=-2.4×10^{-4} cm^3 g^{-1} K^{-1}) were taken from ref 15. On the basis of the unimer formula of $B_{12}E_{260}B_{12}$, the aggregation number (n_w) of the micelle can be computed. We have taken M_w to be close to the true micellar molar mass, since the small refractive index difference between E and B blocks is negligible. The M_w, n_w, and A_2 values obtained are listed in Table 1. It is seen that n_w increases with increasing temperature due to the poorer solubility of mainly the B block with

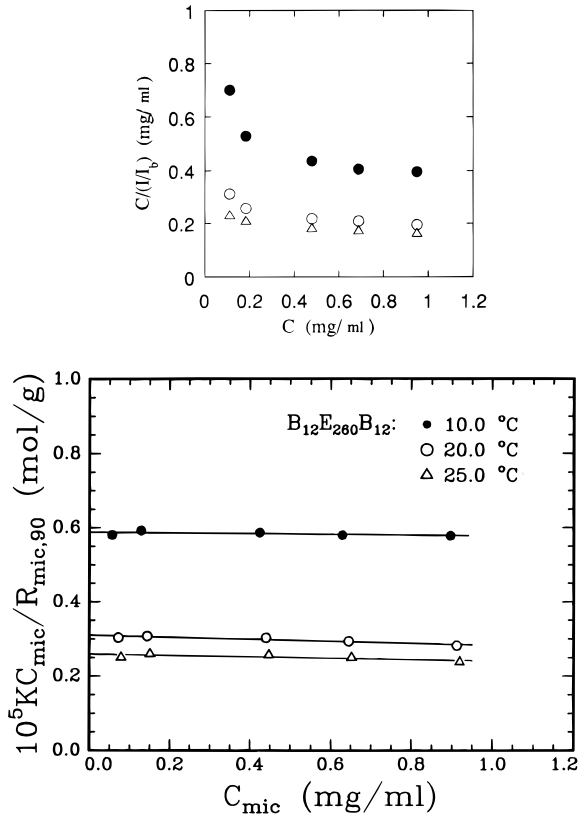

Figure 3. (a) Plot of reciprocal of relative reduced scattered intensity, $C/(I/I_b)$, versus concentrations with $I_b = I_{bz,25}$ of Figure 2. The temperature sequence from top to bottom: 10.0 (filled circles), 20.0 (hollow circles), and 25.0 (hollow triangles) °C. The upturn at low concentrations reinforces the presence of unimers, which has already been illustrated in Figure 2. (b) Plot of $KC_{mic}/R_{mic,90}$ versus micellar concentration (C_{mic}) at 10.0, 20.0, and 25.0 °C. The subscript mic denotes micelle. K is an optical constant, and $R_{mic,90}$ is the excess Rayleigh ratio of the micelle measured at a 90° scattering angle.

Table 1. Micellar Parameters Derived from SLS in the Dilute Region (<1 mg/mL)

temp (°C)	M_w (10^5 g/mol)	n_w	A_2 (cm^3 mol g^{-2})
10.0	1.70 ± 0.01	13	$-(5 \pm 4) \times 10^{-5}$
20.0	3.23 ± 0.03	24	$-(1.4 \pm 0.3) \times 10^{-4}$
25.0	3.86 ± 0.07	29	$-(1 \pm 0.5) \times 10^{-4}$

increasing temperature. Small but negative A_2 values ($\sim 1 \times 10^{-4}$ cm^3 mol g^{-2}), which have been reported for other $B_nE_mB_n$ copolymers,[15,16,20] suggest a possible dangling conformation for some of the end blocks of the $B_{12}E_{260}B_{12}$−water systems.

Dynamic Light Scattering from Dilute Solutions. Figure 4 shows the dynamic light-scattering results in terms of the translational diffusion coefficient (D) (obtained by the CONTIN method) as a function of micellar concentration (C_{mic}) for solutions at 10.0, 20.0, and 25.0 °C. With the relations

$$D_{20°C} = D_{0,20°C}(1 + k_D C_{mic}) \quad (2)$$

and

$$D_0 = kT/(6\pi\eta R_h) \quad (3)$$

the hydrodynamic radius (R_h) can be computed. In order to make proper comparisons, the D value has been normalized to 20 °C, where we used $D_{20°C} = D(\eta/\eta_{20°C})(293.15/T)$ with η and T being the solvent viscosity at temperature T and temperature expressed in K, respectively. The DLS results are listed in Table 2. The hydrodynamic radius increases slightly from 12.0 nm

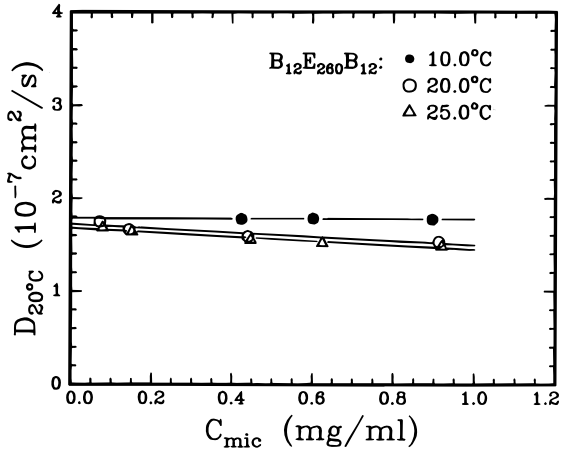

Figure 4. Plot of $D_{20°C}$ versus micellar concentration (C_{mic}). $D_{20°C}$ is the diffusion coefficient which has been corrected to a hypothetical solvent viscosity (H_2O) at 20 °C.

Table 2. Micellar Parameters Obtained from DLS in the Dilute Region (<1 mg/mL)

temp (°C)	$D_{0,20°C}$ (10^{-7} cm^2/s)	R_h (nm)	k_D (cm^3/g)
10.0	1.78 ± 0.01	12.0	−6.8[a]
20.0	1.72 ± 0.03	12.4	−132
25.0	1.68 ± 0.02	12.7	−139

[a] $B_7E_{40}B_7$ gives a k_D value of −6.6 cm^3/g at 20 °C (ref 15), which is comparable with that of $B_{12}E_{260}B_{12}$ at 10 °C.

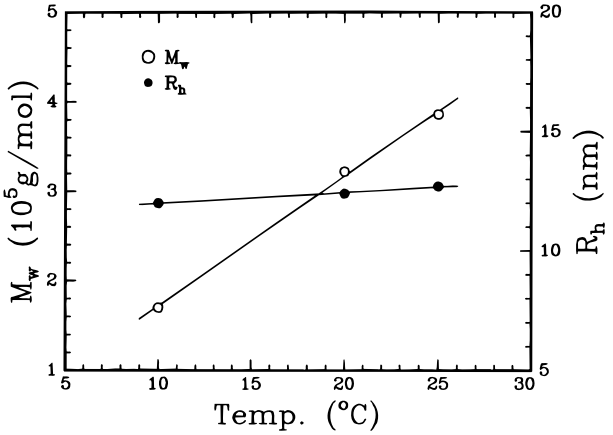

Figure 5. Effect of temperature on M_w and R_h of $B_{12}E_{260}B_{12}$ micelles.

at 10.0 °C to 12.7 nm at 25.0 °C, while the aggregation number (see Table 1) more than doubled from 13 at 10.0 °C to 29 at 25.0 °C. This effect is shown graphically in Figure 5, where both M_w and R_h are plotted against T. The approximate constancy of R_h on increase of temperature has been reported elsewhere.[17,24] As first suggested by Attwood et al.,[24] a constant value of R_h on raising T can be attributed to an increase in n_w being compensated by a contraction of the oxyethylene fringe of the micelle. This explanation is consistent with the negative temperature coefficient of solubility of oxyethylene chains in water and with the importance of the thickness of the fringe in determining R_h.

Thermodynamic Functions of Micellization. For a closed association process to a high aggregation number, the standard free energy ($\Delta G°$) and standard enthalpy of micelle formation ($\Delta H°$) are related to the cmc and its temperature dependence by the relations

$$\Delta G° = RT \ln \text{cmc} \quad (4)$$

$$\Delta H° = R[\text{d} \ln \text{cmc}/\text{d}(1/T)] \quad (5)$$

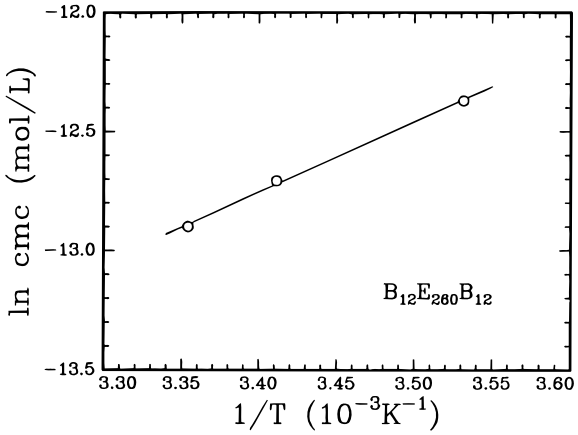

Figure 6. Plot of ln cmc versus the reciprocal of absolute temperature. The least squares fit (solid line) yields $\Delta H°$ based on eq 6.

where the cmc is a molar concentration; $\Delta G°$ and $\Delta H°$ are expressed in energies per mole of solute in the micelle and represent standard states of ideally dilute solution at unit molarity. Equation 5 can be integrated to yield

$$\ln \text{cmc} \simeq \Delta H°/RT + \text{constant} \qquad (6)$$

provided that $\Delta H°$ is independent of temperature. Figure 6 shows a plot of ln cmc (mol/L) versus $1/T$ for $B_{12}E_{260}B_{12}$ in water. From the slope, the standard enthalpy of micellization between 10 and 25 °C was found to be 24.5 ± 1.1 kJ/mol, in contrast to $P_{14}E_{24}P_{14}$ (Pluronic R 17R4) with $\Delta H° = 115 \pm 6$ kJ/mol between 35 and 40 °C.[8] The small $\Delta H°$ value for $B_{12}E_{260}B_{12}$ is consistent with previous values obtained for other E/B copolymers with B-blocks of 10 units or more: e.g., 34 kJ mol^{-1} ($E_{58}B_{17}E_{58}$),[21] 24 kJ mol^{-1} ($E_{40}B_{15}E_{40}$)[22] and 30 kJ mol^{-1} ($E_{24}B_{10}$).[25] In contrast, values of $\Delta H°$ found for E/B copolymers with shorter B blocks (8 units or less) are generally higher: e.g., 80 kJ mol^{-1} ($E_{27}B_7$,$E_{30}B_5$),[26] 95 kJ mol^{-1} ($E_{21}B_8E_{21}$),[13] and 80 kJ mol^{-1} ($B_5E_{91}B_5$).[20] It has been suggested[26] that this apparent anomaly could possibly be attributed to the more tightly coiled configuration for the longer B blocks, so that interaction with water *via* hydrophobic bonding was reduced when compared with that prevailing for the shorter B blocks. However, $\Delta H°$ for the Pluronic polyols, as summarized in ref 7 (see Table 5 therein), increases with increasing P block length and in most cases gives very high values (200−400 kJ mol^{-1}).

CONTIN[18] Analysis. The intensity−intensity correlation function [$G^2(\tau)$] is related to the field correlation [$g^{(1)}(\tau)$] with $G^{(2)}(\tau) = A(1 + b|g^{(1)}(\tau)|^2)$ by using the self-beating technique where A is a baseline and b is the coherence factor. For a polydisperse system,

$$g^{(1)}(\tau) = \int G(\Gamma) e^{-\Gamma\tau}\, d\Gamma \qquad (7)$$

where $G(\Gamma)$ is the normalized characteristic line width distribution function. A Laplace inversion of eq 7 by means of the CONTIN method, together with $\Gamma = Dq^2$ and eq 3, can provide us with information on the size distribution function of micelles in terms of $R_{h,app}$, where we have neglected the intermolecular interactions. Figure 7 shows that for a dilute solution at $C = 0.48$ mg/mL, the apparent hydrodynamic radius ($R_{h,app}$) increases slightly with increasing temperature, as also listed in Table 2. However, at the same time, the width of the size distribution decreases with increasing temperature. Figure 8 shows the concentration effect on

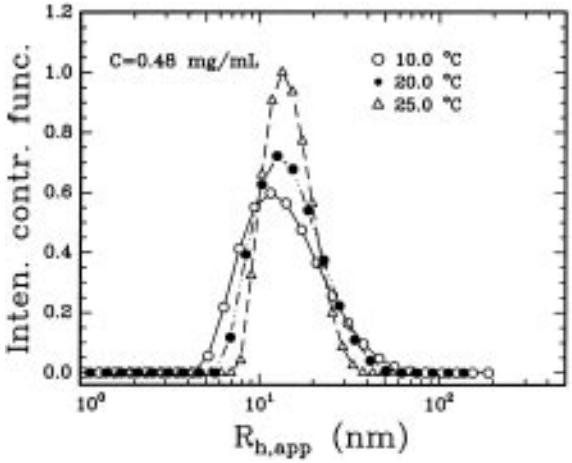

Figure 7. Intensity contribution function versus apparent hydrodynamic radius at 10.0, 20.0, and 25 °C. $C = 0.48$ mg/mL.

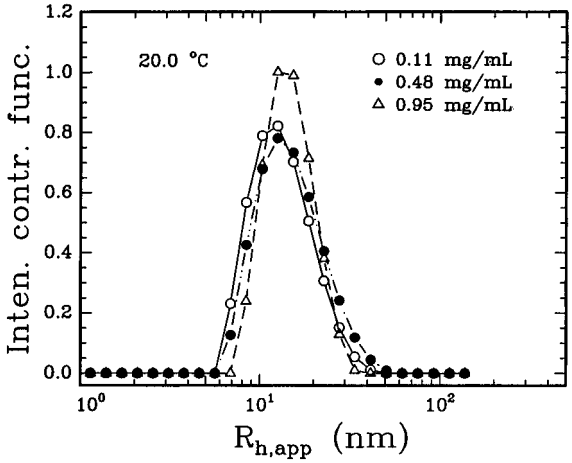

Figure 8. Intensity contribution function versus apparent hydrodynamic radius at 0.11, 0.48, and 0.95 mg/mL and a fixed temperature of 20.0 °C.

$R_{h,app}$ at a fixed temperature of 20.0 °C. The average apparent size increases slightly with increasing concentration, but the width of size distribution remains essentially the same. Both Figures 7 and 8 support the closed association mechanism, implying the formation of flower-like micelles above the cmc in the dilute solution regime.

3. Higher Concentrations (C = 10−20 mg/mL). Figures 9 and 10 show scattered intensity distributions of the apparent hydrodynamic radius (R_h with app deleted from here on for brevity) at concentrations from about 5 to 20.0 mg/mL at 10.0 and 20.0 °C, respectively. For comparison, Figure 9 also includes the results for a dilute solution ($C = 0.95$ mg/mL) at 10 °C. It is noted that the cmc = 0.056 and 0.040 mg/mL at 10.0 and 20.0 °C. In Figure 9, the peaks at low R_h, as have been reported previously,[15,20] showed an increase in R_h and intensity with increasing concentration, suggesting the presence of, most likely, molecular associates under certain conditions.

By comparing Figures 7 and 9, the micellar size distribution at 10 °C remains somewhat broad at concentrations above cmc from 0.48 to ∼10 mg/mL. In this concentration region, the sizes increase moderately with increasing concentration. However, at 20 mg/mL, larger size supramicellar associates seem to increase noticeably, reaching sizes in the 10^2 nm range. At 20 °C (see Figure 10), the secondary association, perhaps in the form of branched and more open structures,

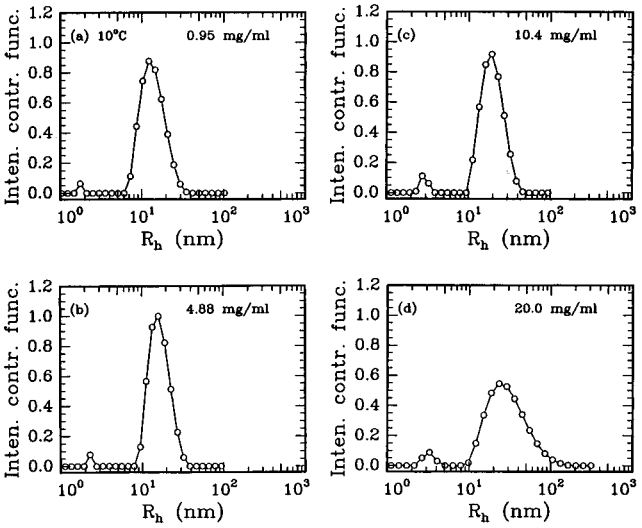

Figure 9. Intensity contribution function versus apparent hydrodynamic radius at 10 °C and different concentrations. C = 0.95, 4.88, 10.4, and 20.0 mg/mL.

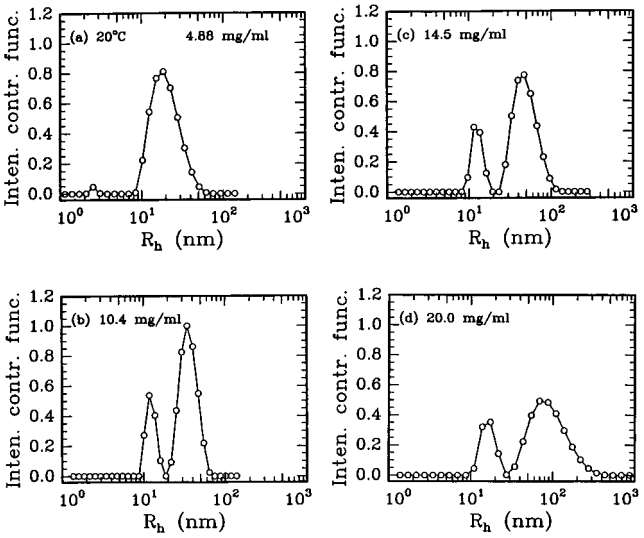

Figure 10. Intensity contribution function versus apparent hydrodynamic radius at 20 °C and different concentrations. C = 4.88, 10.4, 14.5 and 20.0 mg/mL.

becomes increasingly more important at higher concentrations. At C > 10 mg/mL, the secondary association already dominates the DLS peak. However, it should be noted that the actual amount could still be small, as the intensity contribution function is heavily weighted by the large molar mass of the aggregates. At higher concentrations (14.5 and 20.0 mg/mL), the contribution from the secondary association not only increases but the size of the aggregates becomes larger. The CONTIN results at higher concentrations also account for the observation that a 4% $B_{12}E_{260}B_{12}$ aqueous solution is highly viscous with viscosity values of 120, 340, and 780 mPa s at 15.0, 20.0, and 25.0 °C in the shear rate region 0.5−20 s^{-1}, as measured with a Bohlin CS 50 rheometer.

Conclusions

The $B_{12}E_{260}B_{12}$ triblock forms micelles in very dilute solutions (cmc ≃ (3−6) × 10^{-2} mg/mL) even at fairly low temperatures (e.g., 10 °C). Micelle formation in dilute solution obeys a closed association process with the cmc decreasing with increasing temperature. It is interesting to note that the micellar molar mass increases by a factor of ∼2 from 10 to 25 °C, whereas the hydrodynamic size (≃24 nm) remains essentially unchanged over the same temperature range.

The more interesting aspect of the present study is that at room temperatures $B_{12}E_{260}B_{12}$ is able to form large secondary structures at concentrations of only 1−2% (w/v), as clearly shown by Figure 10b−d. The secondary associates, in coexistence with narrowly size-distributed, flower-like micelles, increase in both amount and size with increasing concentration and increasing temperature. This accounts for the highly viscous fluid behavior of a 4% aqueous solution of $B_{12}E_{260}B_{12}$ with the viscosity increasing with increasing temperature.

Acknowledgment. B.C. gratefully acknowledges support of this work by the U.S. Army Research Office (DAAH0494G0053), the National Center for Human Genome Research (1RO 1HG01386-01), and the Human Frontier Science Program (Strasbourg, France). C.B. wishes to acknowledge support by the Science and Engineering Research Council (UK).

References and Notes

(1) Yu, G.-E.; Deng, Y.-L.; Dalton, S.; Wang, Q.-G.; Attwood, D.; Price, C.; Booth, C. *J. Chem. Soc., Faraday Trans.* **1992**, *88*, 2537.
(2) Malmsten, M.; Lindman, B. *Macromolecules* **1992**, *25*, 5440.
(3) Mortensen, K.; Pedersen, J. S. *Macromolecules* **1993**, *26*, 805.
(4) Alexandridis, P.; Holzwarth, J. F.; Hatton, T. A. *Macromolecules* **1994**, *27*, 2414.
(5) Schillen, K.; Brown, W.; Johnson, R. M. *Macromolecules* **1994**, *27*, 4825.
(6) Wanka, G.; Hoffmann, H.; Ulbricht, W. *Macromolecules* **1994**, *27*, 4145.
(7) Chu, B.; Zhou, Z. In *Nonionic Surfactants: Polyoxyalkylene Block Copolymers*; Nace, V. M., Ed.; Marcel Dekker: New York, 1996, Chapter 3.
(8) Zhou, Z.; Chu, B. *Macromolecules* **1994**, *27*, 2025.
(9) Wang, Y.; Mattice, W. L.; Napper, D. *Macromolecules* **1992**, *25*, 4073.
(10) Nguyen-Misra, M.; Mattice, W. L. *Macromolecules* **1995**, *28*, 1444.
(11) Raspaud, E.; Lairez, D.; Adam, M.; Carton, J.-P. *Macromolecules* **1944**, *27*, 2956.
(12) Mortensen, K.; Brown, W.; Jorgensen, E. *Macromolecules* **1994**, *27*, 2654.
(13) Yang, Z.; Pickard, S.; Deng, N.-J.; Barlow, R. J.; Attwood, D.; Booth, C. *Macromolecules* **1994**, *27*, 2371.
(14) Dow Chemical Co., Freeport, TX, Technical Literature, B-Series.
(15) Yang, Y.-W.; Yang, Z.; Zhou, Z.; Attwood, D.; Booth, C. *Macromolecules* **1996**, *29*, 670.
(16) Yang, Z.; Yang, Y.-W.; Zhou, Z.; Attwood, D.; Booth, C. *J. Chem. Soc., Faraday Trans.* **1996**, *92*, 257.
(17) Zhou, Z.; Chu, B. *J. Colloid Interface Sci.* **1988**, *126*, 171.
(18) Provencher, S. W. *Makromol. Chem.* **1979**, *180*, 201; *Comput. Phys. Commun.* **1982**, *27*, 213, 229.
(19) Yang, Y.-W.; Brine, G.; Yu, G.-E.; Heatley, F.; Attwood, D.; Booth, C.; Malmsten, M. *Polymer*, submitted for publication.
(20) Zhou, Z.; Chu, B.; Nace, M. *Langmuir*, in press.
(21) Luo, Y.-Z.; Nicholas, C. V.; Attwood, D.; Collett, J. H.; Price, C.; Booth, C. *Colloid Polym. Sci.* **1992**, *270*, 1094.
(22) Luo, Y.-Z.; Nicholas, C. V.; Attwood, D.; Collett, J. H.; Price, C.; Booth, C.; Zhou, Z.; Chu, B. *J. Chem. Soc., Faraday Trans.* **1993**, *89*, 539.
(23) Deng, N.-J.; Luo, Y.-Z.; Tanodekaew, S.; Bingham, N.; Attwood, D.; Booth, C. *J. Polym. Sci., Part B, Polym. Phys.* **1995**, *33*, 1085.
(24) Attwood, D.; Collette, J. H.; Tait, C. *Int. J. Pharm.* **1985**, *26*, 25.
(25) Bedells, A. D.; Arafeh, R. M.; Yang, Z.; Attwood, D.; Heatley, F.; Padget, J. C.; Price, C.; Booth, C. *J. Chem. Soc., Faraday Trans.* **1993**, *89*, 1235.
(26) Tanodekaew, S.; Deng, N.-J.; Smith, S.; Yang, Y.-W.; Attwood, D.; Booth, C. *J. Phys. Chem.* **1993**, *97*, 11847.

MA9607473